ISSN 22846808

Open Access Journal

Letters in Applied NanoBioScience

Volume 3, Issue 1, 130-143, 2014

www.NanoBioLetters.com

THE STUDY OF THERMAL EFFECTS AND DEFECT MODE PROPERTIES ON THE ONE-DIMENSIONAL PHONONIC BAND GAP STRUCTURES

Arafa H. Aly[1*], Ahmed Mehaney[1]

[1] *Department of Physics, Faculty of Sciences, Beni-Suef University, Egypt*

Article info

Received: 05.03.2014
Accepted: 22.03.2014
Published: 30.03.2014

Abstract

In the present work, we describe an efficient study of the stop-band/pass-band dispersive behavior of 1D phononic crystal. We have treated the propagation and localization of in-plane (P and S)/anti-plane (SH) shear waves in perfect/defect phononic crystals. Based on the transfer matrix method and Bloch theory, the dispersion relations were calculated and plotted for both SH and in-plane waves. In order to confirm the results, the reflection coefficients were plotted for in-plane waves and compared with dispersion relations results. The effect of several parameters such as type and thickness of defect layer on the waves localization had be taken in account. Moreover, we have studied the effect of temperature on the phononic band gaps for SH and in-plane waves. These results can be useful in using phononic crystals as temperature sensor materials. Also, the presented analysis can be extended to acoustic filters and wave multiplexer.

Keywords *stop-band, pass-band,dispersive,1D phononic crystal, localization, in-plane (P and S), anti-plane (SH)*

*Corresponding author e-mail address: **arafa16@yahoo.com**

Introduction

Recently, numerous research papers were focused on the novel materials such as phononic crystals. Phononic crystals (PnCs) are periodic composite structures that offer exceptional control over phonons, sound and other mechanical waves. The PnCs structures commonly consist of a periodic array of two or more materials with different elastic properties. The periodic variation of density and/or elastic constants of the structure changes periodically. This changes the speed of sound in the crystal, which, in turn leads to the formation of the so-called phononic band gaps or stop bands [1-5].Within the band gaps wave propagation is effectively prohibited. Furthermore, the phenomena of negative refraction and acoustic metamaterials have been observed in PnCs [6, 7]. These unusual effects of PnCs can be utilized in a broad range of engineering applications such as transducers, acoustic filters, acoustic wave guides[8], sound collimation[9], acoustic rectification[10], frequency sensing[11,12] and control of vibration isolation. Some PnCs exhibit phononic band gaps for any propagation direction, which are known as complete band gaps. Other crystals exhibit band gaps for only certain direction (partial band gaps), since one_ dimensional crystal possess phononic band gaps for waves that propagate in only one direction [3]. Therefore, PnCs can be classified according to periodicity into three types, i.e., the one- dimensional (1D), the two- dimensional (2D) and the three-dimensional (3D) PnCs [13-17]. Moreover, not all 3D PnCs exhibit complete band gaps, this depends on the structure of composite materials. In order to create a complete band gaps, the crystal structure must possess a band gap for both longitudinal and transverse waves at the same frequency region. The propagation of

mechanical waves in fluids differ than in solids, fluids support only longitudinal polarization, while solid materials can support both longitudinal and transverse polarizations. Based on these different types of polarizations, PnCs can be also classified to three categories; solid/solid structures, solid/fluid structures and fluid/fluid structures [15-21]. These different types of structures and waves polarizations increase the challenges for PnCs rather than photonic crystals, since electromagnetic waves have only transverse polarizations.

So far, several methods were developed to calculate the phononic band gaps such as Plane-Wave-expansion Method (PWM) [22]. But this method fails in some cases such as calculating the dispersion relation for PnCs in mixed solid/fluid structures, where the materials contrast is very high. Also Bloch-Floquet Method (BFM)[23] for studying layered structures, and other methods[24-26]. In this paper the transfer matrix method [27] is adopted, which is particularly suited for 1D problems. Due to its recursive nature, it allows for a repeated enforcement of the continuity conditions at interfaces between materials [28]. It focuses on obtaining the dispersion relations for elastic waves propagation through periodic structures. The results of the dispersion relation represent the band structure of the periodic materials that relates the frequency, ω, and the wave vector, k, of the propagating wave. In general the formation of such a banded frequency spectrum is based on "Bragg reflection" that results in waves interference at interfaces between materials. As result of interference, the destructive interference result in creation of ranges of frequencies known as stop bands or band gaps, over which all incident waves are effectively attenuated. The other frequency bands known as pass bands, constructive interference dominated and waves effectively propagate through the structure [29].

There are several parameters and factors to be considered and they have pronounced effects on the band structure and on the band gaps behavior. Temperature can play an effective role on the properties of the frequency band gaps. For example, at certain frequencies and incident angles, the thermal effects on the refraction direction of PnCs can be changed from negative to positive by varying the temperature on PnCs with air back ground [30]. Moreover, the thermal conduction of phonon transport in silicon PnCs has been reduced to less than 4% of the bulk value for silicon at room temperature [31]. Another factor has attracted increasing interest, is the layer randomness and defect structures. Practical periodic structures are always different than ideal ones because of defaults or manufactures errors. The immersing of defect layer inside the periodic structure affects the band gaps and waves localization in photonic crystals [32]. Therefore, many studies were reported about disordered PnCs [33]. Most of the previous studies were performed on the wave's localization in the pass bands. However, wave's localization in the band gaps must be paid more interest because of its important in the propagation of elastic waves and creation of sharp peaks of transported energy.

The goal of this paper is to provide additional analysis and comprehensive study of the stop-band/ pass-band dispersive behavior of the 1D periodic structure. The transfer matrix method is adopted for this purpose. Based on the transfer matrix method and Bloch theory, the dispersion relations are calculated and plotted for SH- waves propagating in an arbitrary direction. Also this paper focuses on correlating and comparing between the results of SH- waves and in-plane waves propagating normally to the structure. SH- waves are considered as S-waves polarized in the horizontal plane, while in-plane waves consist of S- and P-waves. Also, in order to clarify the results for in-plane waves, the reflection coefficients for S and P- waves are plotted and compared with the dispersion relations curves. Furthermore, in this paper we are interested in studying the effects of temperature on the band structure of PnCs and on the phononic band gap width for both in-plane and SH- waves. Also numerical results are presented and discussed to investigate the effect immersing a defect layer inside the binary periodic structures. Finally, the effects of the thickness and type of the defect layer material on the band gap structure had been discussed.

Theoretical treatment

Basic equations of wave motion. Consider 1D PnCs as shown in Fig.1. The crystal structure consists of infinite number of repeated unit cells. Each unit cell includes two sub-cells made by two different materials *A* and *B*, and denoted by the subscript $j = 1, 2$. The thickness, Lame' constant, shearing modulus, Poisson's ratios, mass density and Young's modulus of the two layers are denoted by $a_j,\ \lambda_j,\ \mu_j,\ \upsilon_j,\ \rho_j,\ E_j [E_j = \lambda_j (1+\upsilon_j)(1-2\upsilon_j)/\upsilon_j]$, respectively. So the thickness of a unit cell (the lattice constant) is $a = a_1 + a_2$.

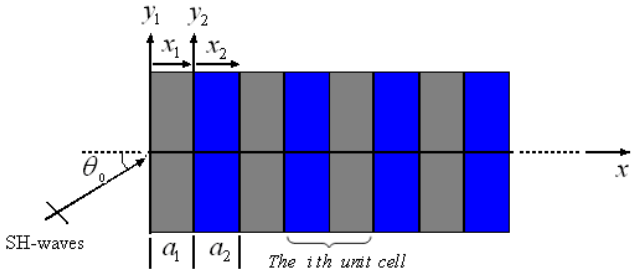

Figure 1: *A schematic diagram of a perfect 1D binary PnCs*

For the case of SH- waves polarized in the z-direction propagating in the xy-plane, the governing equation in each material (layer) can be written in the following form [34-36].

$$\mu_j \nabla^2 \varphi_j(x_j, y_j, t) + \sigma_j^{tx} \frac{\partial^2 \varphi_j^2(x_j, y_j, t)}{\partial x^2} = \rho_j \ddot{\varphi}_j(x_j, y_j, t) \quad (j = 1, 2), \qquad (1)$$

where $\varphi_j(x_j, y_j, t)$ are the displacement components in the z- direction, t the time, T the temperature changes along the x-axis, $\sigma_j^{tx} = E_j \beta_j T/(1-2\upsilon_j)$ the thermal stress component, β_j the thermal expansion coefficients along the x-axis and $\nabla^2 = \partial/\partial x_j^2 + \partial/\partial y_j^2$ the Laplacian operator.

The solution $\varphi_j(x_j, y_j, t)$ in the *j*th layer with time harmonic dependence can be expressed as [37]:

$$\varphi_j(x_j, y_j, t) = \phi_j(x_j) exp[iky_j \sin\theta_0 - i\omega t], \qquad (2)$$

where, $i^2 = -1, k = \omega/c$ is the wave number, ω the angular frequency, c the wave velocity, θ_0 the incident wave angle and ϕ_j the amplitude of the displacements. It will be convenient to introduce the following dimensionless coordinates:

$$\xi_j = x_j/\bar{a}_1, \quad \eta_j = y_j/\bar{a}_1 \quad (j = 1, 2), \qquad (3)$$

where $\bar{a}_1$ is the mean value thickness of material A and it exactly equal to a_1 for the perfectly periodic structure. Substituting Eq. (3) into Eqs. (1) and (2), the following non-dimensional wave equations can be obtained:

$$\varphi_j(\xi_j, \eta_j, t) = \phi_j(\xi_j) exp[i\alpha\eta_j \sin\theta_0 - i\omega t], \qquad (4)$$

$$(1+\chi_j)\frac{d^2\phi_j}{d\xi_j^2} - \alpha^2\left(\sin^2\theta_0 - \frac{\alpha_j^2}{\alpha^2}\right)\phi_j = 0, \qquad (5)$$

where $\alpha = k\bar{a}_1$ is the dimensionless wave number of the incident SH- waves, $\alpha_j = k_j \bar{a}_1$ is the dimensionless wave number in materials A and B, $k_j = \omega/c_j$ is the wave vector in each material, c_j is the wave velocity in each material, $\chi_j = \sigma_j^{tx}/\mu_j$ is the ratio of the stress and shearing modulus in each material. The general dimensionless solution to Eq. (5) is written as a superposition of the forward and backward traveling waves and it is given by the form,

$$\phi_j(\xi_j) = A_j exp(-i\alpha q_j \xi_j) + B_j exp(+i\alpha q_j \xi_j), \quad (j = 1, 2), \qquad (6)$$

where A_j and B_j are unknown coefficient to be determined and q_j is a parameter and has the value $q_j = \frac{1}{\sqrt{1+\chi_j}}\sqrt{c^2/c_j^2 - \sin^2\theta_0}$.

Therefore, the dimensionless solution $\varphi_j(\xi_j, \eta_j, t)$ with time harmonic dependence is:

$$\varphi_j(\xi_j,\eta_j,t)=A_j exp(-i\alpha q_j\xi_j)+B_j exp(+i\alpha q_j\xi_j)\left(exp[i\alpha\eta_j\sin\theta_0-i\omega t]\right) \quad (7)$$

Transfer matrix method for the periodic structure. The dimensionless shear stress component is given by

$$\tau_{xzj}=\mu_j\frac{\partial\varphi_j}{\bar{a}_1\partial\xi_j} \quad (j=1,\ 2). \quad (8)$$

We ssume that the PnCs consist of n unit cells, the boundary conditions at the left and right sides of the two layers in the i th unit cell are written as [35]:

$$\varphi_{jL}^{(i)}=\varphi_j^{(i)}(0),\quad \varphi_{jR}^{(i)}=\varphi_j^{(i)}(\zeta_j),$$

$$\tau_{xzjL}^{(i)}=\mu_j^{(i)}\frac{\partial\varphi_j^{(i)}}{\bar{a}_1\partial\xi_j}(0),\quad \tau_{xzjR}^{(i)}=\mu_j^{(i)}\frac{\partial\varphi_j^{(i)}}{\bar{a}_1\partial\xi_j}(\zeta_j)\quad (i=1,2,....,n), \quad (9)$$

where the subscripts *L* and *R* denote the left and right sides of the two layers, and $0\le\xi_j\le\zeta_j=a_j/\bar{a}_1\quad(j=1,2)$ are the dimensionless thicknesses of materials *A* and *B*. Substituting Eqs. (7) and (8) into Eq. (9) the following matrix equation can be obtained:

$$v_{jR}^{(i)}=T_j^{'}v_{jL}^{(i)}\quad (j=1,\ 2\ ;\ i=1,\ 2,...,\ n), \quad (10)$$

where

$$v_{jR}^{(i)}=\left\{\varphi_{jR}^{(i)},\ \bar{a}_1\tau_{xzjR}^{(i)}\right\}^T \text{ and } v_{jL}^{(i)}=\left\{\varphi_{jL}^{(i)},\ \bar{a}_1\tau_{xzjL}^{(i)}\right\}^T$$

are the dimensionless state vectors at the right and left sides of the two layers and $T_j^{'}$ are 2×2 transfer matrix of the two layers. The elements of $T_j^{'}$ are given by

$$T_j^{'}(1,1)=\frac{\exp(i\alpha q_j\zeta_j)+\exp(-i\alpha q_j\zeta_j)}{2},\ T_j^{'}(1,2)=\frac{\exp(i\alpha q_j\zeta_j)-\exp(-i\alpha q_j\zeta_j)}{2i\alpha q_j\mu_j},$$

$$T_j^{'}(2,1)=\frac{i\alpha q_j\mu_j[\exp(i\alpha q_j\zeta_j)-\exp(-i\alpha q_j\zeta_j)]}{2},\quad T_j^{'}(2,2)=T_j^{'}(1,1). \quad (11)$$

Analysis of the dispersion relation. At the interfaces between the layers, the following condition is satisfied:

$$v_{1R}^{(i)}=v_{2L}^{(i)}. \quad (12)$$

Thus, the relationship between the right and left sides of the i th unit cell can be obtained from Eq. (10) as

$$v_{2R}^{(i)}=T_i\,v_{1L}^{(i)}\quad (i=1,\ 2,...,n), \quad (13)$$

where T_i is the accumulative transfer matrix of the i th unit cell and can be written as *i*

$$T_i=T_2^{'}T_1^{'}. \quad (14)$$

At the interface between the right side of the $(i-1)$th unit cell and the left side of the i th unit cell, the following condition is satisfied:

$$v_{1L}^{(i)}=v_{2R}^{(i-1)}\quad (i=2,....., n). \quad (15)$$

By equating Eq. (13) and Eq. (15), we can obtain the relationship between the state vectors of the $(i-1)$th unit cells and the i th unit cell in the following form:

$$v_{2R}^{(i)}=T_i\,v_{2R}^{(i-1)}\quad (i=2,....., n), \quad (16)$$

so T_i is the transfer matrix between two consecutive unit cells.

Based on the Bloch theorem and Floquet's theorem, due to the periodicity of the layered –component PnCs, the displacement and stress at the boundaries between two neighboring unit cells satisfy the following relations [35, 38]:

$$\varphi_{2R}^{(i)}=\varphi_{2R}^{(i-1)}\exp(ika),\quad \tau_{xz2R}^{(i)}=\tau_{xz2R}^{(i-1)}\exp(ika), \quad (17)$$

where k is the wave number that corresponding to the effective wave field across the periodic medium. Combining the above two equations leads to the following matrix equation:

$$v_{2R}^{(i)}=v_{2R}^{(i-1)}\exp(ika)\quad (i=2,....., n). \quad (18)$$

By equating Eq. (16) and Eq. (18) which leads to the following eigenvalue problem:

$$\left|T_i-e^{ika}I\right|=0. \quad (19)$$

Eq. (19) can be rewritten as

$$T_i\,v_{2R}^{(i-1)}=\lambda\ v_{2R}^{(i-1)}, \quad (20)$$

where $\lambda=e^{ika}$ is a complex eigenvalue and $V_{2R}^{(i-1)}$ is a complex eigenvector. The wave number in Eq.(20) is a complex number, where $k=k_{real}-ik_{imaginary}$ so we have two cases. 1- If $k=k_{real}$ and $k_{real}>0$. The waves are allowed to propagate in the structure at these pass band

frequencies.2-If $k = -ik_{imaginary}$ *and* $k_{imaginary} < 0$, the waves are not allowed to propagate in the structure at theses band gap frequencies.

Temperature effects on PnCs. When mechanical waves propagate through PnCs structure, a compression or rarefaction occurs which may heats or cools the structure. This heat causes thermal expansions, which will affect on the elastic constants of the material. Since the compressions and rarefactions occur very rapidly, there is not time for much heat to flow and the elastic constants measured by sound propagation are the adiabatic constants. The adiabatic constants are related to the isothermal constants by the formula [39, 40],

$$\lambda^{\sigma} = \lambda^{\theta} + \frac{9\beta^2 B^2 \theta}{\rho C_V}, \quad \mu^{\sigma} = \mu^{\theta}, \quad (21)$$

where the superscripts σ and θ indicate adiabatic and isothermal constants, β the thermal expansion coefficient, *B* the bulk modulus $(B = \lambda + 2/3\mu)$, θ the absolute temperature in kelvins, ρ the density, and C_V the specific heat at constant volume.Eq.21 indicates that there is a difference between λ^{σ} and λ^{θ} should be taken in account.

As a consequence, if the temperature increased, not only the elastic constants will change to new values, but also the dimensions of the layers will change according to the relation [41]:

$$\Delta a = \beta a_i \Delta t, \quad (22)$$

since Δa is the change in the layer thickness, a_i is the initial thickness and Δt is the change in temperature. As a consequence, these new parameters will affect the stress parameters in SH- waves equation and in-plane wave velocities as well. Since P-wave velocity is $c_P = \sqrt{\frac{\lambda + 2\mu}{\rho}}$, which, in turn leads to variation of the band structure and band gaps properties as we will investigate in the next section.

Numerical examples and Discussions

In this section the numerical results are performed and discussed for the propagation and localization of elastic waves in both perfect and defect binary PnCs. Special attention is devoted to analyze the effects of temperature on the band structure and band gap parameters. The dispersion relations are studied for the two situations:(1) SH-waves propagation. (2) in –plane waves propagation.

3.1. Results for SH-waves propagation. According to the definition of the periodic structure, the number of unit cells must be infinite, but in numerical practice should take a finite number. So the dispersive behavior of the periodic materials and structures with an arbitrary chosen unit cells configuration is considered as an example. We consider the PnCs made by =4 unit cells (N=8 layers), where each unit cell is composed of two layers. The two layers are lead and epoxy materials and denoted by A and B respectively. The materials constants can be found in [32, 36] and listed in table 1.The wave velocity of the incident wave, , is taken as 800 m/s. The angle of the incident wave is taken as and the temperature is considered as . Since the structure is considered as inhomogeneous structure, the dispersive characteristics are determined by the ratios of materials properties. Hence we consider the thickness ratio of each material is 1:1. Therefore, the thicknesses of materials A or B (and) inside each unit cell are 1/2 of the unit cell thickness, and weight of each unit cell inside the binary crystal is 1/4 of the crystal thickness.

In Fig.2, the dispersion relations are calculated and plotted for SH-waves in the first Brillouin zone by the non- dimensional frequency $q = \omega a / c_B$ versus the non- dimensional wave number $\zeta = k \times a$. Where a is the unit cell length and c_B is the wave velocity in material *B*. The frequency range is taken

as $0 \le q \le 30$. These dispersion relations represent the band structure of the perfect PnCs and can be classified according to Fig.2 as follow. We can see that some frequency regions are plotted with white color (pass-bands regions).

Table 1: *Material constants*

Materials	Mass density $\rho \times 10^3$ (kg/ m^3)	Lame' constant $\lambda \times 10^{10}$ (N/m^2)	Shearing modulus $\mu \times 10^{10}$ (N/m^2)	Young's modulus $E \times 10^{10}$ (N/m^2)	Poisson's ratios ν	Thermal expansion coefficient $\beta \times 10^{-6}$ (1/ ^{o}C)	Specific heat $C_\nu \times 10^3$ (J/kg. ^{o}C)
Pb	11.4	3.3	0.54	1.536	0.43	29.5	0.128
Epoxy	1.180	0.443	0.159	0.435	0.368	22.5	1.182
Al	2.699	6.1	2.5	6.752	0.355	23.9	0.9
Au	19.32	15.0	2.85	8.114	0.42	14.2	0.13
Nylon	1.11	0.511	0.122	0.357	0.4	50	1.70

These frequency regions corresponding to real valued wave number and in which the SH- waves are allowed to propagate through the structure. The other frequency regions are plotted with gray color (stop-bands regions). These regions corresponding to complex or pure imaginary wave number and in which the wave amplitudes decrease exponentially. As a result, the waves cannot propagate through the structure.

3.1.1. Influences of the defect layer on the band structure. In this section, we have studied the effects of immersing a defect layer inside a perfect periodic structure. This layer affects the wave localization inside the band gaps and band structure as we will investigate in this section.

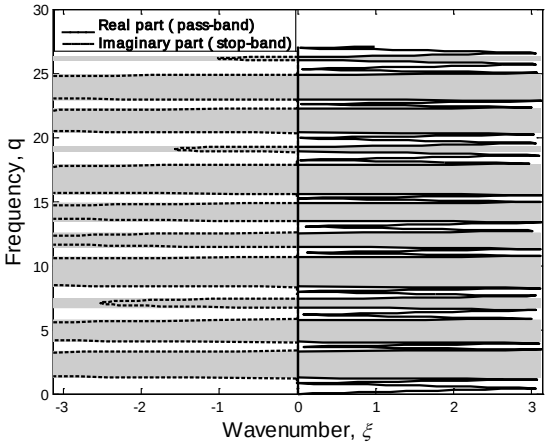

Figure 2:*The calculated dispersion relation curves for SH-waves propagating in an arbitrary direction to 1D binary perfect PnCs consisting of n=4 unit cells (eight layers). Each unit cell consists of lead and epoxy materials. The thickness of each material inside any unit cell is 1/2 of the unit cell thickness, and the unit cell thickness is 1/4 of the structure thickness (stop-bands shaded in gray).*

Consider we have immersed a defect layer of thickness a_d to the perfect ones used in section 2.1 as shown in Fig.3. The transfer matrix of the defect layer is calculated by using Eq. (11). The total transfer matrix T_i in Eq. (19) of the structure is calculated as a dot product of the accumulative transfer matrices before and after the defect with the defect layer transfer matrix T_d as follow

$$T_i = T_n T_{n-1} .. T_d .. T_m ... T_1 \text{ with } T_m = T_2^{'} T_1^{'}$$

and $T_j^{'}$ given in Eq. (11).

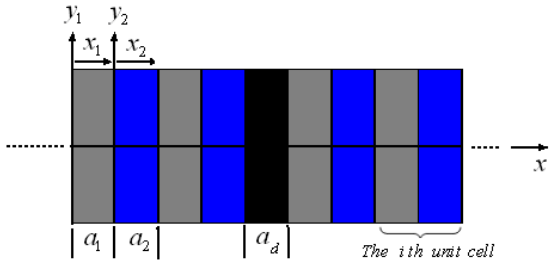

Figure 3: *A schematic diagram of a defect 1D binary PnCs*

Fig.4 shows the effects of the defect layer on the band gap structure. In order to compare the results of the defect structure with those investigated for the perfect ones in section 3.1. We exploited the same materials that had been used in section 3.1with the same ratios

and conditions (*n*=4, $\theta_0 = 10^0, T = 20^0 C$ and $\zeta_1 : \zeta_2$ = 1:1).

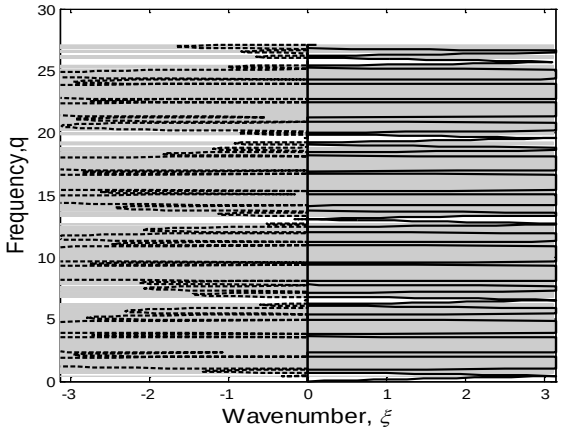

Figure 4: *The calculated dispersion relation curves for SH-waves propagating in an arbitrary direction to 1D binary defect PnCs consisting of n=4 unit cells.*

A defect layer made from aluminum with thickness $a_d = a_A$ was immersed after the second unit cell *(stop-bands shaded in gray).*

We consider a defect layer made from aluminum was immersed after the second unit cell, the material properties are mentioned in table1. We consider the defect layer thickness $a_d = a_A$ i.e. 1/2 of any unit cell thickness. From Fig.4 it can be seen that the wave propagation behaviors and band gap structure changed obviously for the defect structure than the perfect ones. For example, there is an increment in the number and width of the band gaps, also the band gaps and pass bands edges fluctuated to new values due to inserting of a defect layer inside the structure. This layer affects the periodicity of the structure and increase the heterogeneity inside it. As a result, narrow peaks with high purity have appeared inside the band gaps. Therefore, waves localization in the band gaps appear and increase by introducing a defect inside the perfect PnCs. In addition to the related dependence of the wave localization on the defect layer, the thickness of the defect layer can play an important role on the number and width of localized waves. It can be seen from Fig.5 (a and b) that the peaks width decreased by increasing the defect layer thickness, i.e. the peaks width in Fig.5 (b) is smaller than the peaks width in Fig.5 (a). This is because of increasing the contrast at the defect layer boundaries, which leads to increasing of band gaps width and decreasing of pass bands width. More clarification for this point, from Fig.5(c and d) we can see that for the same thickness a_d, the peaks width changed by changing the materials type of the defect layer. In Fig.5(c) we used a material (gold) with elastic constant larger than material *A* or *B*, while in Fig.5 (d) we used a material (nylon) with elastic constants to some extent close to material *A* and *B*. As a result, we can note in Fig.5(c) that the number and width of pass band peaks are smaller than in Fig.5 (d).The nylon material acts as spring between structure materials and introduces local resonance inside structure, which increase the localized waves. This dependence of wave localization on the defect layer can be utilized in multiple channel acoustic filter and wave multiplexer.

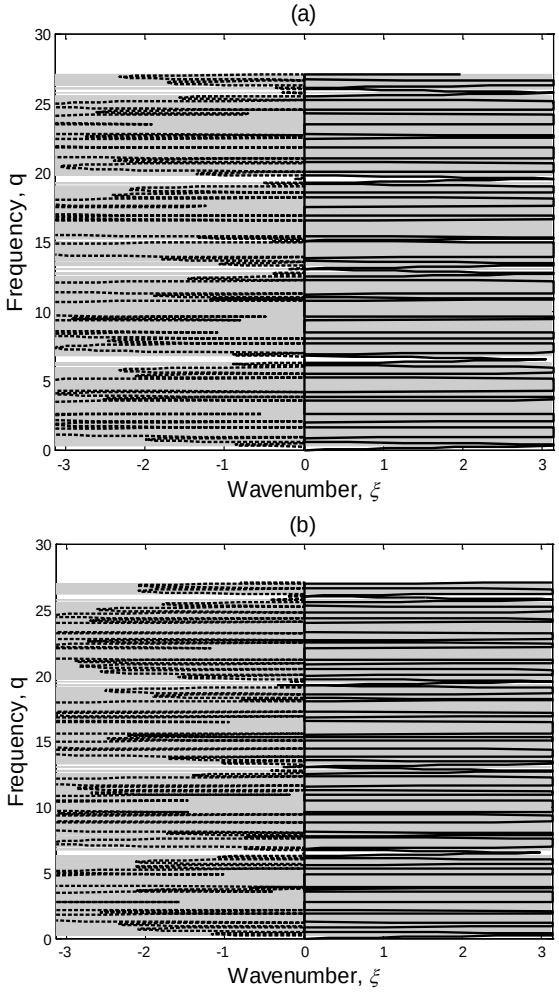

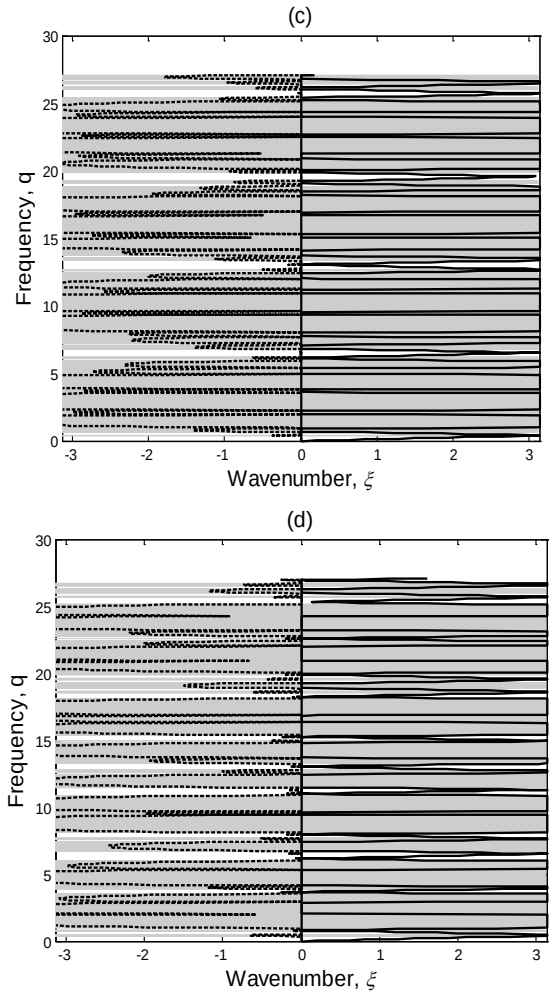

Figure 5: *The calculated dispersion relatrion curves for SH-waves propagating in an arbitary direction to 1D binary defect PnCs consisting of n=4 unit cells.*

(a) Aluminum defect layer with $a_d = 3a_A$,

(b) Aluminum defect layer with $a_d = 5a_A$, (c) Gold defect layer with $a_d = a_A$ and

(d) Nylon defect layer with $a_d = a_A$ *(stop-bands shaded in gray).*

3.1.2. Influence of temperature on the band structure. In order to investigate the influence of the temperature on the band structure and on the band gap parameters, different temperature changes (i.e. T = 50,100,150 and 190^{0}C) are considered. The dispersion relations are calculated with the same materials and conditions (n=8, $\theta_0 = 10^0$ and $\zeta_1 : \zeta_2$ = 1:1).Fig.6 shows the response of the dispersion relations with different temperatures for SH-waves propagation in PnCs. It can be seen that from Fig.6 the pass bands became stop bands and vice versa. From these results, we can that the band gaps effects is not obvious for small temperatures as in Fig.6 (a and b), but the temperature has an obvious effects on the band structure at higher temperatures as in Fig.6 (c and d).By increasing the temperature, some of comment on the possible effects of temperature changes on the band structure of PnCs at SH- wave propagation by the following two results. First, the SH –waves propagation and band gap structure can be tuned by temperature changes. Second, we can note in Fig.6 (a, b, c and d) that the temperature has not great effect on the pass band/stop band width. This saturation of width is due to increasing of the value of thermal stress which has negative value and prevent materials from lengthening. Therefore, the contrast between materials thicknesses remains constant and no variation in the band gaps width.

Also, we can see that the band gap edges decreased slightly toward low values by increasing of temperature. For instance, the band gap at frequency $q = 25$ had decreased to low frequency values as indicated in Fig.6(c and d) compared with Fig.6 (a and b).An interpretative of this decrease is the using of materials with different thermal expansion coefficients, this leads to different thermal stress values in the used materials.

3.2. Results for in-plane waves propagation. In order to compare the dispersion relation results for SH-wave with in-plane wave propagation, Fig.7 presents the dispersion relation for in-plane wave propagates normal to 1D perfect PnCs($\theta_0 = 0^0$).We consider the same PnCs structure in section 3.1 with the same materials and conditions n=8 and $\zeta_1 : \zeta_2$ = 1:1 (i.e. $a_A = a_B$ *=1/2* unit cell thickness). The eigen value problem in Eq.(19) can be easily extended for plane wave propagation. The elements of the transfer matrix in Eq. (11) for longitudinal wave (P-wave) and transverse wave (S-wave) can be deduced by the same analysis procedure and can be found in [30]. In Fig.7

the dispersion relations are calculated for the plane waves in the first Brillouin zone by the non-dimensional frequency q :(q range is $0 \le q \le 30$, $q = q_{PB} = \omega a / c_{PB}$ and $q = q_{SB} = \omega a / c_{SB}$ for P and S waves respectively) versus the non-dimensional wave number $\zeta = k \times a$.

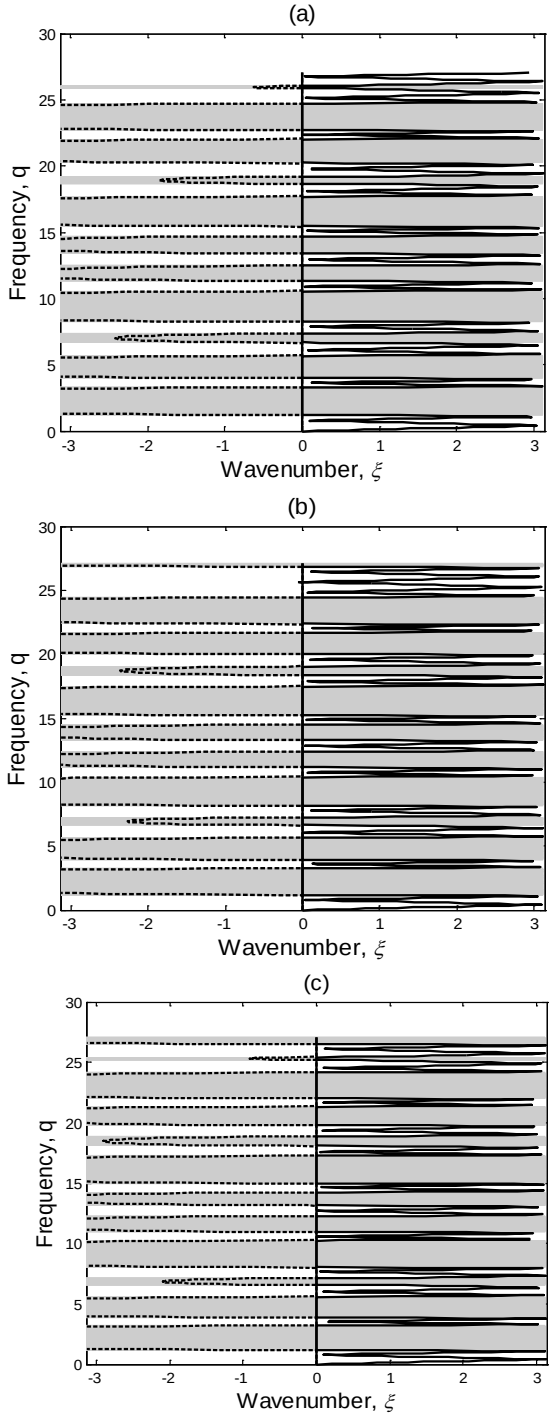

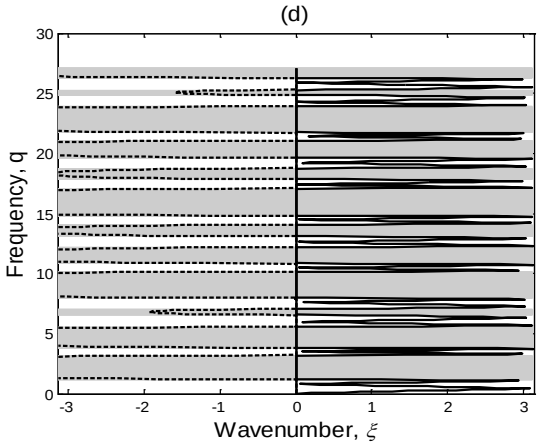

Figure 6: *The calculated dispersion relation curves for SH-waves propagating in an arbitrary direction to 1D binary perfect PnCs consisting of n=4 unit cells. Each unit cell consists of lead and epoxy materials. Different temperatures are considered. (a) T = 50^{0}C, (b) T =100^{0}C, (c) T= 150^{0}C and (d) T =190^{0}C, respectively (stop-bands shaded in gray).*

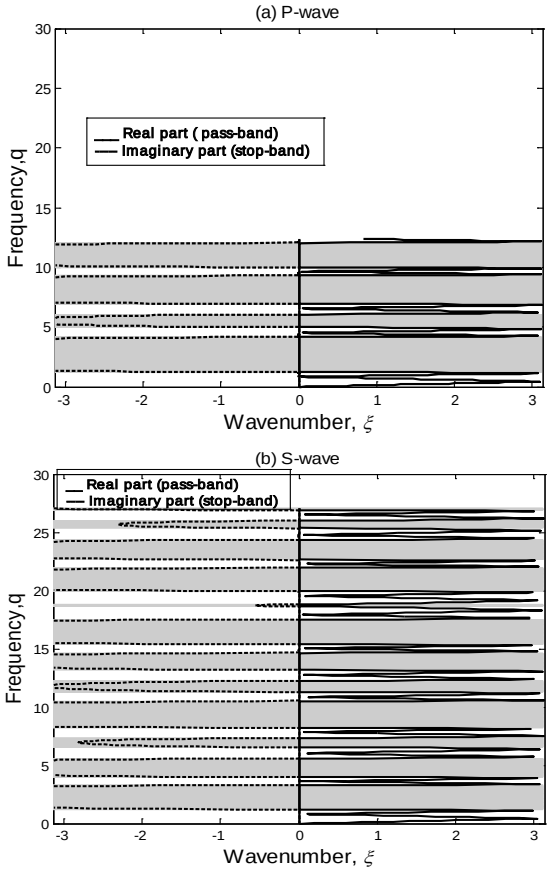

Figure 7: *The calculated dispersion relation curves for in-plane wave propagates normal to 1D binary perfect PnCs consisting of n=4 unit cells (eight layers). Each unit cell consists of lead and epoxy materials. (a)P-wave and (b) S-wave (stop-bands shaded in gray).*

Where c_{PB} and c_{SB} are the longitudinal and transverse wave velocities in the second material *B* respectively, and ***a*** is the unit cell length. The difference and excess in band gaps values between S-wave than P-wave is due to the difference between P and S- waves velocities. P- waves depend on both the compression and shear properties of the material, while S- waves depend on the shear properties only. The common frequency band gaps for P and S- waves represent the complete band gap for in-plane waves. In order to confirm these results for plane waves, we calculated the reflection coefficient for P and S- waves in the *x* direction through *N*=8 layers bonded to semi infinite materials (nylon material) at the two ends. As depicted in Fig.1, the reflection coefficient based on the transfer matrix method given in the following. The sub-scripts "0" and "e" will be denoting the left and the right semi- infinite materials, respectively.

When a plane wave propagates to the layer, the reflection coefficient for the displacement field is given by [33]

$$\frac{U_1}{U_0} = \frac{T_{12} + E_0 T_{11} - E_0 E_e T_{21} - E_e T_{22}}{E_0 (T_{11} - E_e T_{21}) - (T_{12} - E_e T_{22})}, \quad (23)$$

where U_1 is the reflected amplitude and $T_{ij} = T(i, j)$ are the elements of the total transfer matrix; $T = T_n T_{n-1} \ldots T_m \ldots T_1$. Fig.8 gives the relation between the reflectance *R* versus $\omega a / 2\pi c_T$ ($c_T = c_{SB}$) for P-wave (gray dashed lines) and S-wave (black solid lines) [42]. From Fig.8 we can identify the frequency ranges for which the reflectance of normal incident P and S- waves is high (e.g. $R > 0.99$). These high reflectance at different frequency ranges represents the frequency band gaps for P and S – waves in the PnCs. From Fig.8 it can be seen that the frequency band gaps described by the reflection coefficient are congruent and show good agreement with those described by the dispersion relations. The common frequency regions at $R > 0.99$ for P and S- waves represent the complete band gaps for plane waves in PnCs.There is a simple difference in the band gaps edges between Figs. 7 and 8, and this is due to the relation in Fig.8 is plotted between the reflectance and $\omega a / 2\pi c_T$,since $c_T = c_{SB}$ is chosen for both P and S - waves reflectance.

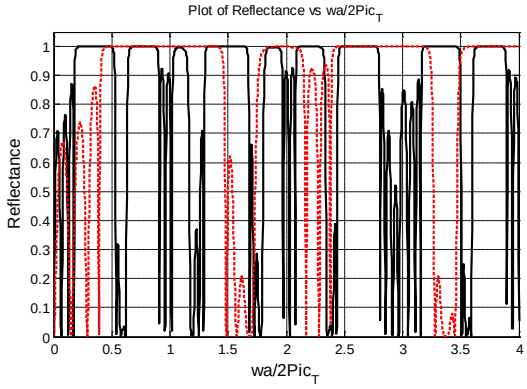

Figure 8: *A plot of reflectance R versus* $\omega a / 2\pi c_T$ *for normal incident P- wave (dotted lines) and S- waves (solid lines) on 1D PnCs consisting of n=4 unit cells (eight layers). Each unit cell consists of lead and epoxy materials.*

3.2.1. Influence of the defect layer and temperature on the band structure "at in- plane wave propagation".

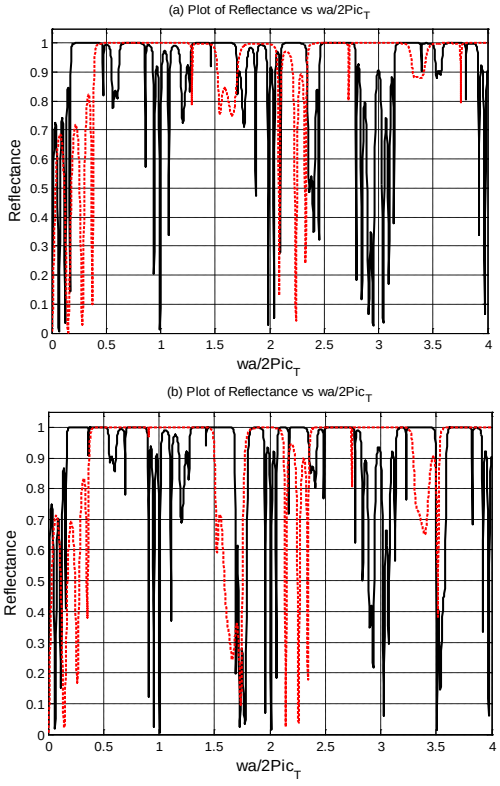

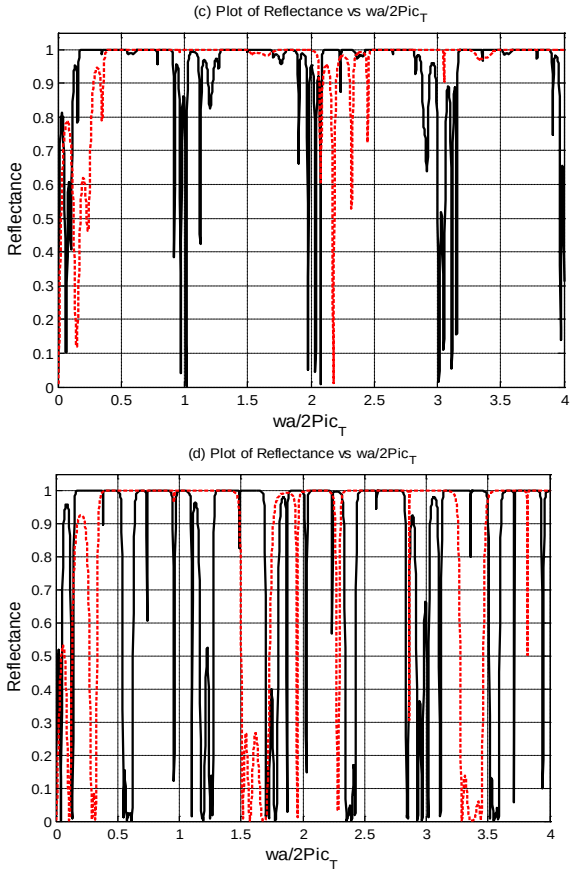

Figure 9: *A plot of reflectance R versus* $\omega a / 2\pi c_T$ *for normal incident P- wave (dotted lines) and S- waves (solid lines) on 1D defect PnCs consisting of n=4 unit cells (eight layers), each unit cell consists of lead and epoxy materials. The defect layer was immersed after the second unit cell.*

(a)Aluminum defect layer with $a_d = a_A$,

(b) Aluminum defect layer with $a_d = 3a_A$,

(c) Gold defect layer with $a_d = a_A$ *and*

(d) Nylon defect layer with $a_d = a_A$.

In this section we will compare between the effects of the defect layer and temperature on the propagation of plane waves through the band structure with those investigated in the previous sections for SH-waves propagation.

3.2.1.1. Influence of the defect layer on the band structure. First, we will use the same defect structure used in section 3.1.1 with the same materials and conditions except the angle of incidence $\theta_0 = 0^0$. From Fig. 8 we have seen that the band gaps that have been described by the reflection coefficient agreed with dispersion relations results. Therefore, we will use the reflection coefficient to describe the effects of the defect layer and temperature instead of dispersion relations in order to plotting both P and S -waves in the same graph.

It is observed from Fig. 9 that the defect layer has pronounced effect on plane wave propagation through PnCs.These results are similar to the results that had been investigated for SH-waves propagation, since there are many peaks of the localized waves had been produced inside the band gaps. The number of the localized waves have increased by increasing defect layer thickness as in Fig.9 (b). Also this number have increased when we used an nylon layer with low elastic constant as in Fig.9 (d) and decreased when we used a gold layer as in Fig.9(c).These results confirm the previous results in section 3.1.1 and congruent with it in the same analysis.

3.2.1.1. Influence of temperature on the band structure.

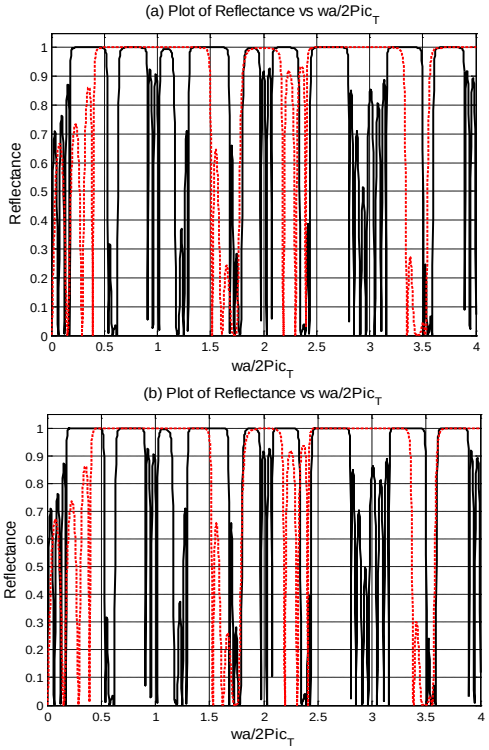

Fig.10. *A plot of reflectance R versus* $\omega a / 2\pi c_T$ *for normal incident P- wave (dotted lines) and S- waves (solid lines) on 1D perfect PnCs consisting of n=4 unit cells (eight layers), each unit cell consists of lead and epoxy materials. Different temperatures are considered. (a) T =* 50^0*C and (b) T =*190^0*C.*

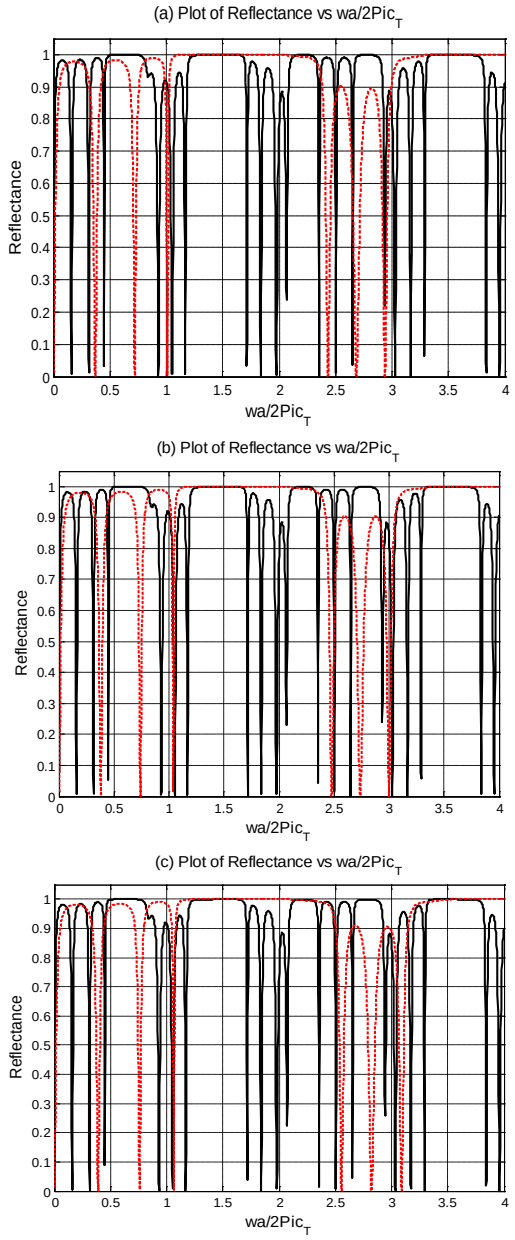

Figure 11: *A plot of reflectance R versus* $\omega a / 2\pi c_T$ *for normal incident S- waves (solid lines) and P- wave (dotted lines) on 1D perfect PnCs consisting of n=4 unit cells (eight layers), each unit cell consists of aluminum and gold materials. Different temperatures are considered: (a) T = 20^{0}C, (b) T =300^{0}C, and (c) T =700^{0}C.*

By the same procedure that used in section 3.1.2 we will investigate the effects of temperature on the band structure at plane wave propagation in order to compare between the two cases. So we will consider the same structure that have been used in section 3.1.2 with the same materials and conditions (*n*=8, $\theta_0 = 0^0$ and $\zeta_1 : \zeta_2 = 1:1$). We prefer to consider the two temperature changes T = 50 and 190^{0}C to illustrate the clear effects of temperature on the band gap structure. Fig. 10 reveal that the temperature has a significant effect on the band gap structure at plane wave propagation through PnCs. For example, if we compared these results with SH-waves results in Fig.8,we can note in Fig.10 (a) that the reflectance of P-wave (dotted lines) shifted toward higher values of the non dimensional frequency $\omega a / 2\pi c_T$ (i.e. band gap at $\omega a / 2\pi c_T$ =3.5). These effects increase by temperature increasing from T = 50^{0}C to T =190^{0}C as indicated in Fig.10 (b). The different effects of temperature on the band structure between SH-wave and in- plane wave are back to two reasons. First, the temperature has direct effect on the elastic constants and P-wave velocity, these effects result in changing the edges and values of the complete band gaps. Second, the absence of the thermal stress and increment of lattice constants as discussed in Eq. (22) result in variation of the band gap values as well. The influences of temperature on the band gap structure can be appear more clearly when we use high melting point materials at the higher temperatures as shown in Fig.11. From these results, several factors related to temperature will be change. For instance, the thermal conduction in silicon PnCs [31] can be change according to these results, where the dispersion relations depend on the frequency band gap values.

Conclusions

In this paper, we have studied the propagation and localization of SH-waves and in-plane waves inside 1D PnCs. The transfer matrix method based on Bloch theory is adopted for this purpose. Furthermore, we have studied the effects of two parameters on the band structure; the first is the effect of a defect layer on the band structure and on the waves localization for both SH-waves and in-plane waves. The second is the effect of temperature on the band structure and on the band gaps parameters for the two waves. In order to confirm

the results, the reflection coefficient is calculated and plotted for in-plane waves. As we expected, the results described by the reflection coefficient agreed with those described by dispersion relations. Therefore, we can use the dispersion relations curves as a good tool to describe the band structure and band gap studies. We can summarize the analyses and discussions in the following results: (1) The defect layer has pronounced effect on the band structure and on the number of localized waves for both SH and plane waves. Also the thickness and type of the defect layer material have an obvious effect on the width and on the number of resonant defect peaks, where the localized waves increased by using a defect layer material with low elastic constant. Also the number of waves increases by increasing the defect layer thickness. The study of wave localization based on the defect layer facilitates the wave localization techniques and can be used to take advantage from manufacture errors. Also it can be utilized in many potential application as acoustic filter, acoustic waveguides and can be applied to produce new types of laser called phonon laser with low thermal effects especially in the hypersonic PnCs regime. (2) The temperature has direct effect on PnCs, especially at plane wave propagation, where P-waves velocities and lattice constants have influenced by temperature increasing. These direct influences on PnCs by temperature can be useful in using PnCs as a temperature sensor. When temperature is increased in PnCs, the phononic sensors band gap experiences a significant change.

References

[1]T. Gorishyy, M. Maldovan, C. Ullal and E.Thomas, Sound ideas, *Physics world December*, 24-29, **2005**.

[2] Arafa H. Aly, Ahmed Mehaney, and Hassan S. Hanafey Phononic Band Gaps in One Dimensional Mass Spring System, *Progress In Electromagnetics Research Symposium Proceedings, KL, MALAYSIA, March 27-30*, 155**, 2012**.

[3]M.N.armenise, C.E.Campanella, C.Ciminelli, F.dell'Olio and V.M.N.passro,Photonic and phononic band gap structures: modeling and applications, *Physics Procedia*, 3, 357-364, **2010**.

4- Arafa H Aly and Ahmed Mehaney, "Enhancement of phononic band gaps in ternary/binary structure, *Physica B: Condensed Matter*, 407, 21, 4262-4268, **2012**.

5- Arafa H Aly and et al "Study of physical parameters on the properties of phononic band gaps, *International Journal of Modern Physics B*, 27, 1350047- 1350062, **2013**.

[6] D.Torrent and J.Safnchez-Dehesa, Radial wave crystals: Radially periodic structures from anisotropic metamaterials for engineering acoustic or electromagnetic waves, *Physical Review Letters*, 103, 064301,1-4, **2009**.

[7]L.Fok and X.Zhang, Negative acoustic index metamaterial, *Physical Review B*, 83, 214304, 1-8, **2011**.

[8] A. Khelif, A. Choujaa, S. Benchabane, B. Djafari-Rouhani, and V. Laude, Guiding and bending of acoustic waves in highly confined phononic crystal waveguides**,** *Applied Physics Letters*, 84,4400,1-3 ,**2004**.

[9] J. Christensen, A. I. Fernandez-Dominguez, F. de Leon-Perez,L. Martin-Moreno, and F. J. Garcia-Vidal, Collimation of sound assisted by acoustic surface waves, *Nature Physics*, 3, 851-852, **2007**.

[10] A. Petri, A. Alippi, A. Bettucci, F. Craciun, F. Farrelly and E. Molinari, Vibrational properties of a continuous self-similar structure, *Physical Review B*, 49,15067-15075, **1994**.

[11] I. El-Kady, R. H. Olsson III, and J. G. Fleming, Phononic band gap crystals for radio frequency communications, *Applied Physics Letters*, 92, 233504, 1-3, **2008**.

[12] S.Mohammadi, A. A. Eftekhar,W. D. Hunt, and A. Adibi, High-*Q* micromechanical resonators in a two-dimensional phononic crystal slab, *Applied Physics Letters*, 94, 051906,1-3, **2009**.

[13] J.J. Chen and X.Han, The propagation of Lamb waves in one-dimensional phononic crystal plates bordered with symmetric uniform layers, *Physics Letters A*, 374, 3243-3246, **2010**.

[14]A. Chen, Y. Wang, G. Yu, Y. Guo and Z. Wang, Elastic wave localization in two-dimensional phononic crystals with one-dimensional quasi-periodicity and random disorder, *Acta Mechanica Solida Sinica*, 21, 517-528, **2008**.

[15]D.Torrent and J. Sanchez-Dehesal, Acoustic resonances in two-dimensional radial sonic crystal shells, *New Journal of Physics*, 12, 073034, 1-19, **2010**.

[16] Z. Liu, X. Zhang, Y. Mao, Y.Y. Zhu, Z. Yang, C.T. Chan and P. Sheng, Locally resonant sonic materials, *Science*, 289, 1734–1736, **2000**.

[17]M.S.Kushwaha, P.Halevi, G.Martinez, L.Dobrzynski, B.Djafari-Rouhani, Theory of acoustic band structure of periodic elastic composities, *Physical Review B*, 49, 2313-2322, **1994**.

[18] E.L. Tan, Generalized eigenproblem of hybrid matrix for Floquet wave propagation in one-dimensional phononic crystals with solids and fluids, *Ultrasonics*, 50, 91-98, **2010**.

[19] Y. Pennec,B. Djafari-Rouhani,J. O. Vasseur,A. Khelif, and P. A. Deymier, Tunablefiltering and demul tiplexing in phononic crystals with hollow cylinders, *Physical Review E*, 69,046608,1-6, **2004**.

[20]R.Lucklum,J.Li and M.Zubtsov, 1D and 2D phononic crystal sensors, *Procedia Engineering*, 5, 436-439 **2010**.
[21] D. Zhao, W. Wang, Z. Liu, J. Shi, W. Wen, Peculiar transmission property of acoustic waves in a one-dimensional layered phononic crystal, *Physica B*, 390,159-166, **2007**.
[22] X.Zhang, Y.Y.Liu, F.G.Wu and Z.Y.Liu, Large two-dimensional band gaps in three-component phononic crystals, *Physics Letters A* 317,144-149, **2003**.
[23]C.Ciminelli,F.Peluso and M.N.Armenise, Modelling and design of two-dimensional guided-wave photonic band-gap devices, *IEEE.Journal of Light wave Technology* 23,886-901, **2005**.
[24]A.Taflove,Computational Electrodynamics:The Finite-Difference Time –Domain method, *Artech House Inc,Norwood,MA*, **1995**.
[25]D.L.Dwoyer,M.Y.Hussaini and R.G.Voigt, Finite Element-Theory and Application, *Spriger-Verlag, New York*, **1986**.
[26] H.G.Zhao, Y.Z.Liu, J.H.Wen, D.L.Yu and X.S.Wen, Tri-component phononic crystals for underwater anechoic coatings, *Physics Letters A*, 367, 224-232, **2007**.
[27]Thomson, W. T., Transmission of elastic waves through a stratified solid medium, *Journal of Applied Physics*, 21, 89–93, **1950**.
[28]L.Liu and M. I. Hussein, Wave motion in periodic flexural beams and characterization of the transition between Bragg scattering and local resonance, *Journal of Applied Mechanics*, 79, 011003,1-17, **2012**.
[29] M. I. Hussein, K. Hamza, G. M. Hulbert,R. A. Scott,K. Saitou, Multiobjective evolutionary optimization of periodic layered materials for desired wave dispersion characteristics, *Structural Multidisciplinary Optimization*, 31, 60–75, **2006**.
[30] L.Y. Wu, W.P. Yang, L.W. Chen, The thermal effects on the negative refraction of sonic crystals, *Physics Letters A*, 372, 2701-2705, **2008**.
[31] P. E. Hopkins,L. M. PhInney,P. T. Rakich,R. H. Olsson III, and I. EL-Kady, Phonon considerations in the reduction of thermal conductivity in phononic crystals, *MeTA'10 2nd International conference on metamaterials, photonic crystals and plasmonics*, 308-316, **2010**.
[32]Arafa .H.Aly and H.A.Elsayed, Defect mode properties in one-dimensional photonic crystal, *Physica B* 407, 120-125, **2012**.
[33] A.L. Chen and Y.-S. Wang, Study on band gaps of elastic waves propagating in one-dimensional disordered phononic crystals, *Physica B*, 392, 369–378, **2007**.
[34] J.L. Rose, Ultrasonic waves in solid media, *Cambridge University Press, London*, **1999**.
[35] Y.Z. Wang, F.M. Li, K. Kishimoto, Y.H. Wang and W.H. Huang, Wave localization in randomly disordered layered three-component phononic crystals with thermal effects, *Archive of Applied Mechanics* 80, 629-640, **2010**.
[36] F.L. Shang, Z.K.Wang, Z.H. Li, An exact analysis of thermal buckling of piezoelectric laminated plates, *Acta Mechanica Solida Sinica*, 10, 95–107, **1997**.
[37] F.M.Li, and Y.S Wang, Study on wave localization in disordered periodic layered piezoelectric composite structures, *International Journal of Solids Structures*, 42, 6457–6474, **2005**.
[38] M. I. Hussein, G. M. Hulbert, R. A. Scott, Dispersive elastodynamics of 1D banded materials and structures: analysis, *Journal of Sound and Vibration*, 289,779-806, **2006**.
[39] D. E. Gray, D. N. Fischel, H. B. Crawford, D.A. Douglas, and W.C.Eisler,
American Institute of Physics Handbook, *Third Edition, Colonial Press, McGraw-Hill Book Company* ,**1972**.
[40] W.P.Mason, Piezoelectric crystals and their application to Ultrasonics, *pp. , D. Van Nostrand Company, Inc., Princeton, N.J, 480-481*, **1950**.
[41] R. A. Serway and J. W. Jewett, Physics for scientists and engineers, *6th Edition, Thomson Brooks/Cole* ,**2004**.
[42]M.Maldovan and E.L.Thomas, Periodic materials and interference lithography for photonics, phononics and mechanics, *Wiley-vch Verlag GmbH and Company KGaA, Weinheim*, **2009**.